IN-33
86838
P.6

NASA Technical Memorandum 105624

Defect Behavior, Carrier Removal and Predicted In–Space Injection Annealing of InP Solar Cells

I. Weinberg and C.K. Swartz
Lewis Research Center
Cleveland, Ohio

and

P.J. Drevinsky
Phillips Laboratory
Bedford, Massachusetts

Prepared for the
Fourth International Conference on Indium Phosphide
and Related Materials
cosponsored by the IEEE and LEOS
Newport, Rhode Island, April 20–24, 1992

NASA

DEFECT BEHAVIOR, CARRIER REMOVAL AND PREDICTED IN-SPACE INJECTION ANNEALING OF InP SOLAR CELLS

I. Weinberg and C.K. Swartz
National Aeronautics and Space Administration
Lewis Research Center
Cleveland, Ohio 44135

P.J. Drevinsky
Phillips Laboratory
Bedford, MA 01731

Abstract

Defect behavior, observed by DLTS, is used to predict carrier removal and the effects of simultaneous electron irradiation and injection annealing on the performance of InP solar cells. For carrier removal, the number of holes trapped per defect is obtained from measurements of both carrier concentrations and defect concentrations during an isochronal anneal. In addition, from kinetic considerations, the behavior of a dominant defect during injection annealing is used to estimate the degradation expected from exposure to the ambient electron environment in geostationary orbit.

Introduction

Radiation induced carrier removal is believed to be a significant factor in affecting the performance of InP solar cells (1). In addition, annealing by minority carrier injection (2) should play a significant role in determining the performance of these cells in space. In both cases, the observed effect is believed to be directly related to the behavior of radiation induced defects. However, attempts to relate carrier removal to specific defect behavior have been admittedly speculative (1). With respect to injection annealing, there have been no published results utilizing defect behavior to predict the effects of injection annealing under the low radiation fluxes typical of the space environment. Hence, one objective of the present work lies in using specific defect behavior to predict carrier removal rates. A second objective lies in using defect behavior to predict annealing of InP solar cells by minority carrier injection in the space radiation environment.

Carrier Removal

Experimental: DLTS and carrier concentration measurements were carried out, after 1 MeV electron irradiation, on small mesa diodes which had been processed on the same wafer next to InP solar cells by MOCVD (3). The DLTS and carrier concentration data relevant to the present case are shown in figure 1. The numbers following the hole trap designations H3, H4 and H5 are the respective defect activation energies as measured in electron volts from the top of the valence band. Carrier removal rates, after 1 MeV electron irradiations were independently determined for similarly processed InP solar cells (4). All cells and diodes were processed by the Spire corporation. Additional details can be found in the cited refs.(3, 4).

Analysis: For a p-type semiconductor, Rc the carrier removal rate is obtained from the relation

$$Rc = \Delta p/\phi \qquad (1)$$

where Δp is the reduction in hole concentration due to irradiation at the fluence ϕ. In general, the measured Δp could be attributable to charge compensation and/or the trapping of holes by radiation induced defects. Assuming that the trapping mechanism is predominant, the carrier removal rate is expressed by the relation

$$Rc = \sum_j IjTj \qquad (2)$$

with $Ij=Nj/\phi$ and $Tj=Pj/Nj$ where Ij is the introduction rate of the jth defect whose concentration is Nj at the radiation fluence ϕ and Pj is the concentration of holes trapped by the jth defect.

Values for the introduction and trapping rates are obtained from the data of figure 1. From the figure it is seen that variations in carrier concentration correspond to changes in defect concentration during the course of the anneal. For example; at T > 200°C. an increase in hole concentration coincides with a decrease in the concentration and eventual disappearance of H5. In this case, the concentration of holes trapped by H5 is obtained from the jump in hole concentration. In a similar manner, the abrupt jump in hole concentration at $T \sim 100°C$ is correlated with the coincident decrease in the concentration of H3 and H4 and the increased concentration of H5. Introduction rates are obtained from the post irradiation defect concentrations and the fluence ($5X10^{15}$ cm^{-2}) cited with the figure. In addition, examination of figure 1 at T > 300°C indicates the presence of residual trapped holes coincident with the almost complete disappearance of all three defects. This is interpreted as indicating the trapping of the residual holes by unannealed defects which are not observed by the present DLTS measurements. These latter carriers are included in the carrier removal calculations by adding the term $P(res)/\phi$ to equation 2 where P(res) is the unannealed carrier concentration at T > 300°C. The results are shown in Table I. In Table II the carrier removal rates, calculated using the data of Table I, are compared with independently measured values for InP solar cells (4). It is seen that there is reasonable agreement between the calculated and independently measured values. Hence, although additional data would be helpful, the present results tend to confirm the use of simultaneous DLTS and carrier concentration measurements during isochronal annealing in predicting values for carrier removal rates. In addition, the trapping rates shown in Table I indicate that the H5 defect, when present at sufficiently high concentration, can be more effective as a hole trap than either H3 or H4. In the present case, the low post irradiation concentration of H5 tends to reduce its effectiveness as a recombination or trapping center. However, it is found that the post irradiation concentration of this defect is observed to increase with increasing dopant concentration while the concentration of the remaining defects decreases. In fact, at a base dopant concentration of $10^{17} cm^{-3}$, the concentration of H5 exceeds that of H4 (5). Hence, at and above this concentration H5 could be more effective than either H3 or H4 in affecting the performance of InP solar cells after 1 MeV electron irradiation.

Injection Annealing

It is known that considerable annealing of radiation induced degradation can be achieved by minority carrier injection, at room temperature, into p-type InP (2). In fact, some cell recovery has been observed when the cell was illuminated during irradiation. Hence, one would expect annealing in space, due to minority carrier injection, to be a major factor in alleviating the effects of radiation induced degradation. To determine the extent of this effect, one needs to perform simultaneous annealing while irradiating the cells at the low radiation fluxes encountered in space. A terrestrial experiment, duplicating the low fluxes observed in space, is impractical because of the extremely long times involved. Instead, we use a kinetic argument to estimate the effects of simultaneous irradiation and annealing in space.

Following Heinbockel et al, the production rate of the jth defect is given by (6)

$$dNj/dt = fj\sigma_d N_a(d\phi/dt) - WjNj \qquad (3)$$

where σ_d is the cross section for atomic displacement, N_a is the concentration of atoms, $d\phi/dt$ is the radiation flux, Wj is the probability per unit time for annealing of the jth defect and fj is the fractional concentration of defect Nj. At equilibrium dNj/dt is zero. Hence from equation 3,

$$Nj = \sigma_d N_a \phi_{ej} \qquad (4)$$

$$\text{with } \phi_{ej} = fj(d\phi/dt)/Wj \qquad (5)$$

ϕej is defined as the effective fluence for production of the jth defect. In general, the effective fluence is the radiation fluence which would produce the equillibrium defect concentration in the absence of annealing (6). In the present case we concern ourselves with the post irradiation defect and preirradation carrier concentrations typical of those in the tables. In that case, H4 is considered to be the dominant defect in reducing cell output (1). Hence, evaluation of the effective fluence for H4 should result in an estimate of cell degradation in a specific orbit. In the present case, we evaluate an effective fluence for a satellite in geostationary orbit.

To evaluate Wj we use the relation obtained for injection annealing of H4 (2),

$$W_{inj} = 19.35 \, J \exp-(E_A/kT) \qquad (6)$$

where J is the cell current density in A/cm2, E_A=0.133 eV is the activation energy for injection annealing (2). The temperature T=333 K is chosen as characteristic of arrays in Geo. Using these values with $J=3X10^{-2}$ A/cm^2 it is found that $W_{inj}=5.64X10^{-3}$ sec^{-1}. It is noted that we consider only injection annealing in the present case. This is justified by noting that, at this temperature, $W_{inj} >> W_{th}$ where the latter is the probability per unit time for thermal annealing (7).

The greatest uncertainty lies in obtaining values for the flux. This is estimated from a compilation of radiation measurements in space where integral electron fluxes in Geo are listed over the energy range from 0.04 to 7 MeV (8). An upper limit to the flux is obtained by using the "worst case" integral fluence ($4.64X10^7$ cm^{-2} sec-1) for electron energies greater than 0.04 MeV (8). Hence, using f=0.7, we obtain $\phi_{e4}=5.8X10^9$ cm^{-2} as the upper limit for the effective fluence due to electron irradiations in geostationary orbit. At this fluence, no cell degradation is expected (1). However one needs to be cautious in interpreting this result. Although steady state (or ambient) electron irradiations dominate over the ambient proton irradiations in Geo, the intermittent proton irradiations associated with solar flares are significant components of the space radiation environment (8). Although statistical models can be used to obtain rough estimates of the effects of solar flares, insufficient DLTS data exists to enable inclusion of the effects of solar flares on the effective fluence. However, the present results are significant in the sense that electron irradiations predominate over protons in the ambient environment of this particular orbit.

Conclusion

Due to the controversy associated with identifying the atomic constitution of the defects observed by DLTS (5, 9) we have avoided designation of submicroscopic structures with the presently observed defects. However, it has been shown that hole trapping and carrier removal can be related to the behavior of specifically labelled defects. Defect behavior has also been used to estimate the performance of InP solar cells under simultaneous injection annealing and electron irradiation in geosynchronous orbit.

References

1. I. Weinberg, Solar Cells 31, p. 331 (1991).
2. M. Yamaguchi, K. Ando, A. Yamamoto and C. Uemura, J. Appl. Phys. 58, p. 568 (1985).
3. P.J. Drevinsky, C.E. Caefer and C.J. Keavney, Proceedings 3rd Int'l. Conf. on InP and Related Materials, p. 56 (1991).
4. I. Weinberg, H.B. Curtis, C.K. Swartz, D.J. Brinker, P.P. Jenkins and M. Faur, Proceedings 22nd IEEE Photovoltaic Spec. Conf. 1991, to be Published.
5. M. Yamaguchi and K. Ando, J. Appl. Phys. 60, p. 935 (1986).
6. J.H. Heinbockel, E.J. Conway and G.A. Walker, Proceedings 14th Photovoltaic Spec. Conf., p. 1085 (1980).
7. M. Yamaguchi and K. Ando, J. Appl. Phys. 63, p. 5555 (1988).
8. E.G. Stassinopoulis and J.P. Raymond, Proceedings of the IEEE 76, p. 1423 (1988).
9. A. Sibile, J. Suski and M. Gilleron, J. Appl. Phys. 60, p. 595 1986.

Table I: Introduction and Trapping Rates Used in Calculating R_c

[c]Hole Conc.	Introduction Rates			Trapping Rates			P(Res)/ϕ
cm^{-3}	cm^{-1}						cm^{-1}
	I_3	I_4	I_5	T_3	T_4	T_5	
[a]2.55×10^{16}	0.88	1.7	0.01	0.63	0.62	3.1	1.1
[b]4.1×10^{16}	0.82	1.2	0.04	0.63	0.62	3.1	1.1

[a] From Fig. 1; [b] Intro. Rates from Ref. 3; [c] Error = ±5%

Table II: Calculated and Measured Carrier Removal Rates

[c]Hole Concentrations	Carrier Removal Rates	
cm^{-3}	cm^{-1}	
	[a] Calculated	[b] Measured
2.4×10^{16}	2.7	2.8
3.9×10^{16}	2.5	2.4

[a] From Table I; [b] Independently Meas. (Ref. 4); [c] Error = ± 5%

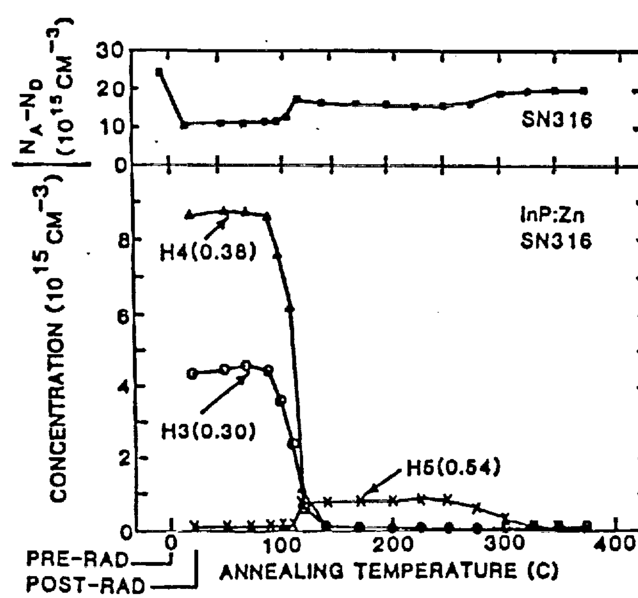

Figure 1. Isochronal Anneal After 1 MeV Electron Irradiation (ϕ=5X10^{15}/cm^2)

REPORT DOCUMENTATION PAGE

Form Approved
OMB No. 0704-0188

1. AGENCY USE ONLY *(Leave blank)*

2. REPORT DATE
1992

3. REPORT TYPE AND DATES COVERED
Technical Memorandum

4. TITLE AND SUBTITLE
Defect Behavior, Carrier Removal and Predicted In-Space Injection Annealing of InP Solar Cells

5. FUNDING NUMBERS
WU-506-41-11

6. AUTHOR(S)
I. Weinberg, C.K. Swartz, and P.J. Drevinsky

7. PERFORMING ORGANIZATION NAME(S) AND ADDRESS(ES)
National Aeronautics and Space Administration
Lewis Research Center
Cleveland, Ohio 44135-3191

8. PERFORMING ORGANIZATION REPORT NUMBER
E-6963

9. SPONSORING/MONITORING AGENCY NAMES(S) AND ADDRESS(ES)
National Aeronautics and Space Administration
Washington, D.C. 20546-0001

10. SPONSORING/MONITORING AGENCY REPORT NUMBER
NASA TM-105624

11. SUPPLEMENTARY NOTES
Prepared for the Fourth International Conference on Indium Phosphide and Related Materials cosponsored by IEEE and LEOS, Newport, Rhode Island, April 20–24, 1992. I. Weinberg and C.K. Swartz, NASA Lewis Research Center; P.J. Drevinsky, Phillips Laboratory, Bedford, Massachusetts 01731. Responsible person, I. Weinberg, (216) 433-2229.

12a. DISTRIBUTION/AVAILABILITY STATEMENT
Unclassified - Unlimited
Subject Category 33

12b. DISTRIBUTION CODE

13. ABSTRACT ***(Maximum 200 words)***

Defect behavior, observed by DLTS, is used to predict carrier removal and the effects of simultaneous electron irradiation and injection annealing of the performance of InP solar cells. For carrier removal, the number of holes trapped per defect is obtained from measurements of both carrier concentrations and defect concentrations during an isochronal anneal. In addition, from kinetic considerations, the behavior of the dominant defect during injection annealing is used to estimate the degradation expected from exposure to the ambient electron environment in geostationary orbit.

14. SUBJECT TERMS
Solar cells; Indium phosphide; Carrier removal; Injection annealing

15. NUMBER OF PAGES
6

16. PRICE CODE
A02

17. SECURITY CLASSIFICATION OF REPORT	18. SECURITY CLASSIFICATION OF THIS PAGE	19. SECURITY CLASSIFICATION OF ABSTRACT	20. LIMITATION OF ABSTRACT
Unclassified	Unclassified	Unclassified	